SYNTHESIS AND CHARACTERIZATION OF HYDROXYAPATITE NANOPARTICLES AND ITS ADSORPTION PARAMETERS FOR ZN(II) AND REACTIVE YELLOW 4 DYE IN AQUEOUS SOLUTION

E. A. Ofudje[1&2]*, A. I. Adeogun[2], M. A. Idowu[2] and S. O. Kareem[3]

[1]*Department of Chemical Sciences, McPherson University, P.M.B. 2094, Abeokuta, Ogun State*, Nigeria.
[2]*Department of Chemistry, Federal University of Agriculture, Abeokuta*, Ogun State, Nigeria.
[3]*Department of Microbiology, Federal University of Agriculture, Abeokuta*, Ogun State, Nigeria.
*Corresponding author: ofudjeandrew4real@yahoo.com, ofudje@gmail.com

Received 16 March 2018; accepted 26 May 2018, published online 23 June 2018

Abstract

The uptake of Zn(II) ions and reactive yellow 4 (RY4) dye from aqueous solutions onto synthesized hydroxyapatite (HAp) nanoparticles was investigated under different experimental conditions such as contact time, initial pollutants concentration, adsorbent dosage, temperature and solution pH, while the structural elucidation of the prepared adsorbent before and after adsorption was achieved using Fourier infrared spectroscopy (FTIR), X-Ray Diffraction (XRD), X-Ray Dispersed Spectroscopy (EDAX), Scanning Electron Microscopy (SEM) and Transmission Electron Microscopy (TEM). XRD results revealed the main characteristic peaks of single phase HAp powder, while the presence of PO_4^{3-}, CO_3^{2-} and OH^- functional groups corresponding to pure HAp were exhibited in the FT-IR analysis. The SEM and TEM analyses confirmed the microscopic morphology of the synthesized apatites to be round shape apatite. The correlation factors R^2 (0.992, 0.992, 0.992 and 0.976) for Zn(II) ions and (0.993, 0.990, 0.994 and 0.993) for RY4 dye obtained from Langmuir, Freundlich, Tempkin and Dubinin-Radushkavich isotherms respectively confirmed the applicability of these models and suggest good agreement between theoretical values and experimental results. Kinetic evaluations showed that the adsorption mechanism obey the pseudo-first-order model with rate constant increasing with initial pollutant concentration. The values of enthalpy change (ΔH) and entropy change (ΔS) as obtained are 4.92×10^6 kJ/mol and 51.123 kJ/mol for Zn(II) ions and 3.99×10^6 kJ/mol and 41.803 kJ/mol for RY4 dye respectively. The valuesof free energy and enthalpy changes revealed that the adsorption process was spontaneous and endothermic in nature. The present study thus concludes that HAp is a good adsorbent for zinc ions and RY4 dye removal from wastewater.

Keywords: Adsorption, equilibrium, hydroxyapatite, kinetic, thermodynamic

Introduction

Increased population, industrialization and extraction of natural resources have resulted in large scale of environmental contamination and pollution. Large amounts of toxic wastes have been discharged into contaminated sites spread across the world [1]. The whole globe is being exposed to contaminants from past and present industrial practices, emissions in natural resources (air, water and soil). Wastewater from the industry is a complex mixture of many polluting substances ranging from dye to heavy metals which are associated with painting, adhesive and the dyeing process [1]. Wastewater from dye industries has been the target of considerable attention in the field of wastewater treatment, not only because of its toxicity, but also because of its visibility [2-3]. The release of these pollutants into the ecosystem endangers human and animal health and also affects the general physiology of plants, because of their toxicity, mutagenicity and non-biodegradability [2]. Over the years, many conventional methods for the removal of pollutants in effluents and wastewater have been discussed and they include physical, chemical and biological processes which include elimination by adsorption, coagulation by

chemical agents, oxidations by ozone or hypochlorite, electrochemical method, membrane separation, ion-exchange, coagulation/flocculation [4-5]. Some of these methods do not actually eliminate contaminants completely; while sometimes they are very expensive and could generate other waste pollutants as secondary products [4-5]. Of these methods however, adsorption has been described as the most eco-friendly and cheap means of pollutants elimination. Thus, several adsorbents such as maize husk [6], coir [7], groundnut husk [8] and activated carbon from bagasse [9] had been demonstrated for their ability to adsorbed pollutants from contaminated environment.

Hydroxyapatite $Ca_{10}(PO_4)_6(OH)_2$, has received extensive attention for its use as an excellent adsorbent for bone filler and implant material due to its biocompatibility prosperity [10]. Hydroxyapatite (HAp) is one of the apatite minerals with a major inorganic constituent with about 60-70 % of the inorganic portion of the bone matrix and possesses high ability of ion-exchange against various cations which make it highly biocompatible, bioactive and as an adsorbent [11-12]. Besides, HAp can be used in a wide range of applications such as bone substitution, food supplements (as a source of calcium), dental materials, drug delivery agent, gene carriers biology, adsorbent in liquid chromatography and proteins, catalysts, ion exchangers, gas sensors, proton conductors and many more [13]. Hydroxyapatite is often used as suitable adsorbent due to its low water solubility, high stability under reducing and oxidizing conditions, high specific surface area, and good buffering properties. The adsorption mechanisms may include ion exchange, adsorption, dissolution–precipitation, and substitution of Ca^{2+} ions in apatite by other metals during co-precipitation [14].The expectation is to combine the excellent sorption property and high chemical stability of the hydroxyapatite as well as the cheap and nontoxic properties of apatite for effective removal of pollutants from aqueous solution. The work aimed at evaluating the feasibility of using chemically synthesized hydroxyapatite (CHM-HAp) powder for the removal of zinc ions and reactive yellow 4 dyes (RY4) from aqueous solution via batch adsorption process under different experimental conditions such as contact time, pollutants concentration, adsorbent dosage and solution pH.

Materials and Methods

Materials

Chemicals

All experiments were performed with analytical reagent grade chemicals and solvents. The reagents that were used for the synthesis of adsorbent were calcium nitrate tetrahydrate (Sigma Aldrich, USA), ammonium dihydrogen phosphate (Sigma Aldrich, USA) and ammonia solution (Loba safety Jar, India).

Synthesis of Hydroxyapatite

The adsorbent was prepared according to the method described by Kaygili and Tatar [10]. Briefly, solution of 0.1 M $Ca(NO_3)_2.6H_2O$ and 0.06 M $(NH_4)H_2PO_4$ were prepared by dissolving 5.90 g and 1.73 g respectively in separate 250 ml deionized water. The aqueous solution of $(NH_4)H_2PO_4$ was added to $Ca(NO_3)_2.6H_2O$ solution drop wise room temperature with continuous stirring on a magnetic stirrer for 24 hours. The solution pH was adjusted to 10 using NH_4OH solution. The gelatinous precipitate was then filtered and centrifuged for 15 mins at 4000 rpm. Thereafter, the sticky filter cake was dried in an oven at 100 °C 24 h. The dried powders were crushed by using mortar and pestle.

Characterization

Fourier Transform Infrared (FT-IR) spectroscopy investigations of the various functional groups presents in the HAp powders were carried out using TENSOR 27, series FT-IR spectrometer, Germany. The KBr pellet technique was used. The phase and purity of the fabricated HAp powders were determined by X-ray diffraction (XRD) using X-pert PRO, PANalytical, Netherland diffractometer (wavelength = CuKα1). The various peaks developed were confirmed by standard Joint Committee of Powder Diffraction Society

(JCPDS) file no: 09-432. Information regarding the surface morphology of the synthesized HAp powders was achieved by scanning electron microscope using a Hitachi (Japan) S-3000H electron microscope with an accelerating voltage with transmission electron microscope (TEM; Tecnai 20 G2 FEI, Netherland). The selected area electron diffraction was also taken. The particle size distribution was determined with Nanotrac equipped with Microtrac FLEX 10.5.2 software. . The zero point charge (P_{ZPC}) of HAp was determined using the method described by Ezechi *et al.* [15].

ADSORPTION EXPERIMENTS

Preparation of Adsorbate Solutions

Stock solution of each of Zn(II) and reactive yellow 4 dye were prepared by dissolving 1 g equivalent of the metal ions and 1 mg of dye in 1 L de-ionized water. The stock solutions were subsequently diluted when necessary to prepare the desired concentration. The prepared dye solution was kept in dark to prevent light degradation.

Batch Adsorption Study

The synthesized hydroxyapatites were used as adsorbents for the removal of Zn(II) and reactive yellow 4 in a batch process. The batch adsorption experiments were carried out in 250 ml Erlenmeyer flasks containing 25 ml of several adsorbate concentrations ranging from 40 to 240 mg/L and 0.04 g of adsorbent on a rotator shaker at 150 rpm and 45 ^{o}C for 120 minutes to reach equilibrium. The solution were separated from the adsorbent and filtered immediately and the filtrate solution was analyzed using Atomic Absorption Spectrophotometer for Zn(II) ions or UV-vis spectrophotometer for reactive yellow 4. The effect of pH, initial adsorbate concentration, adsorbent dosage and temperature on adsorption capacity of the prepared HAp was studied by varying each parameter. The amount of adsorbate adsorbed by various adsorbents was calculated from the differences between initial of 15kV. Elemental composition of the synthesized HAp powders was evaluated with the equipped EDAX. Detailed information about morphological and particle size measurement of the synthesized HAp powders were examined concentration added to the adsorbent and that of the supernatant concentration using the following equations:

$$q_e = \frac{C_o - C_e}{m} \times V \qquad (1)$$

Where q_e is the amount of adsorbate adsorbed, C_o is the initial concentration in mg/L, C_e is the equilibrium concentration in mg/L, 'V' is volume in litre and 'm' is the mass of the adsorbent.

While the percent adsorption is given as:

$$\%\,\mathrm{Re}moval = \frac{C_o - C_e}{C_o} \times 100 \qquad (2)$$

For the reactive dye, the percentage adsorption was estimated using the equation below:

$$\%\ \text{adsorption} = \frac{Abs_o - Abs_e}{Abs_o} \qquad (3)$$

Where Abs_o is the blank absorbance and Abs_e is the absorbance at equilibrium.

Results and Discussions

Table 1: Physical parameters of synthesized HAp

Parameters	HAp
Surface area (m^2/g)	95.17
Average pore Size (nm)	1.24
Pore volume (cm^2/g)	0.43
Bulk density (g/cm^2)	2.97
pH_{ZPC}	6.75

The physical property of the synthesized hydroxyapatite powder was evaluated and the results are as presented in Table 1. The surface area, pore volume, average pore size and bulk density were obtained to

be 95.17 m^2/g, 0.43 nm, 1.24 cm^2/g and 2.97 g/cm^2 % respectively. Fig. 1a shows the representative FT-IR spectra of chemically synthesized HAp, after Zn adsorption and RY4 dye adsorption. Characteristic peaks which appeared at 1084 and 1020 cm^{-1} and the bands noted at 605 and 588 cm^{-1} were assigned to the phosphate groups. The absorption peaks observed between 3640 cm^{-1} were assigned to the stretching vibration of OH^- groups. Furthermore, the stretching band at 3325 cm^{-1} and 1645 cm^{-1} correspond to the stretching vibration of H_2O molecule. The peaks observed at 1465 and 876 cm^{-1} were assigned to CO_3^{2-} group thus suggesting a B-type carbonated HAp [16], which could have originated from atmospheric air. The FT-IR spectra of HAp after the adsorption of Zn(II) ions and RY4 dye showed a similar structure with the synthetic HAp, however, slight changes in the shapes and intensities of the peaks were detected in the PO_4^{3-}, CO_3^{2-} and OH^- functional groups suggesting the incorporation of the pollutants onto the structure of the HAp.

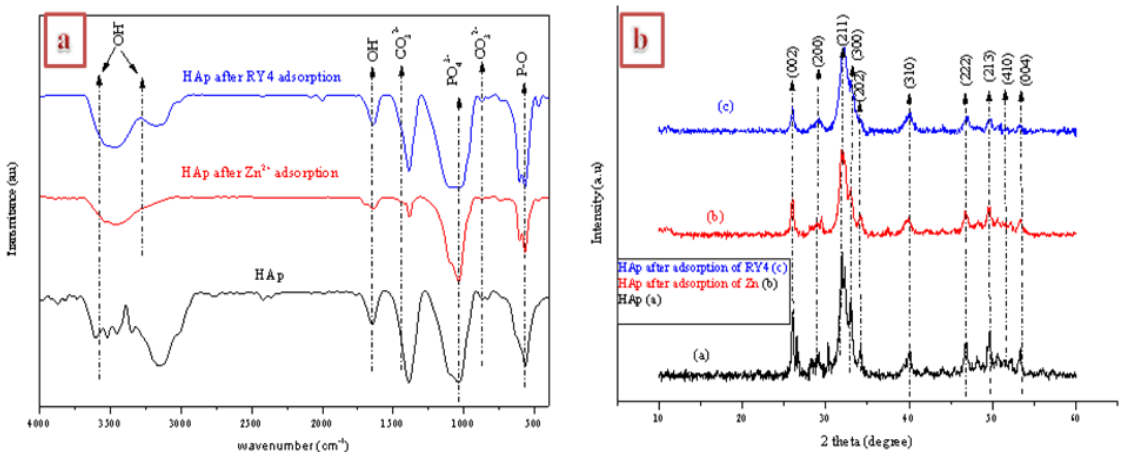

Fig.1: (a) FT-IR and (b) XRD spectra of HAp before and after the adsorption of Zn(II) and RY4 dye.

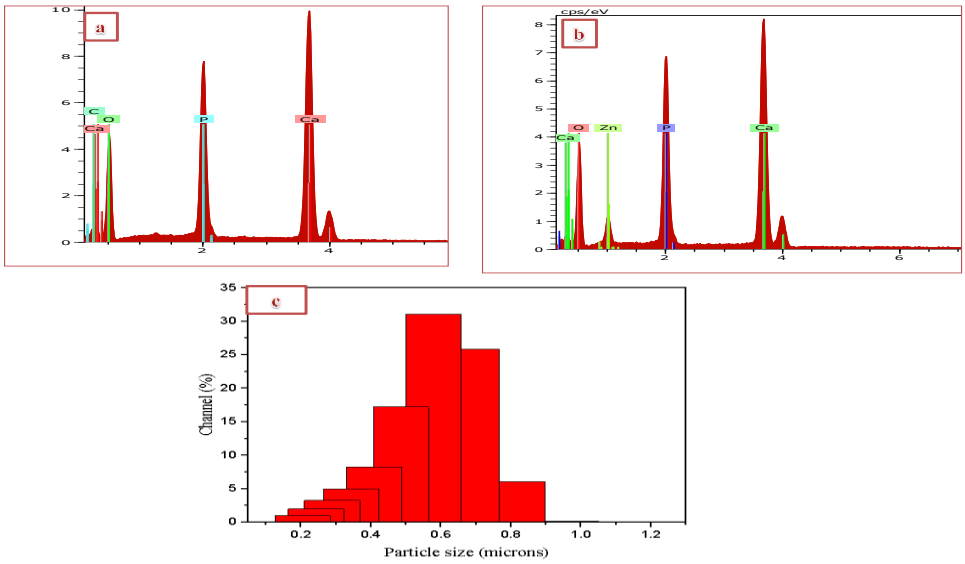

Fig. 2: (a) EDAX of HAp synthesized chemically, (b) EDAX of HAp after adsorption of Zn(II) ions and (c) Particle size distribution of HAp

The XRD patterns of the synthesized HAp and after Zn RY 4 dye adsorption are shown in Fig.1b. The result presents a hexagonal HAp powder when compared with standard JCPDS file no. 09-0432. The most prominent diffraction peaks such as (002), (211), (310) and (213) planes corresponds to HAp were detected. No other unwanted peaks were observed in the apatite after adsorption of the respective pollutants. However, after the adsorption of the process, the peaks become broaden and which decreases in intensities, indicating reduced crystallinity, due to pollutants incorporation onto the apatite [16-18].

Fig.2a depicts the elemental analysis of the prepared HAp showing the distributions of O(62.60 %), Ca(22.05 %), P(11.73 %) and C(3.62 %). However, after Zn(II) ions adsorption, the composition revealed that O(59.42 %), Ca(23.09 %), P(11.77 %) and Zn(5.71 %) as represented in Fig.2b. The Ca/P ratio obtained was 1.88 and 1.96 for pure HAp and after adsorption respectively indicating a non-stoichiometric apatite. Fig.2c shows the particle size distribution of the nanoparticle to be in the range of 0.2 to 0.8 microns.

The surface morphology of the adsorbent before and after adsorption by SEM is as presented in Fig.3.

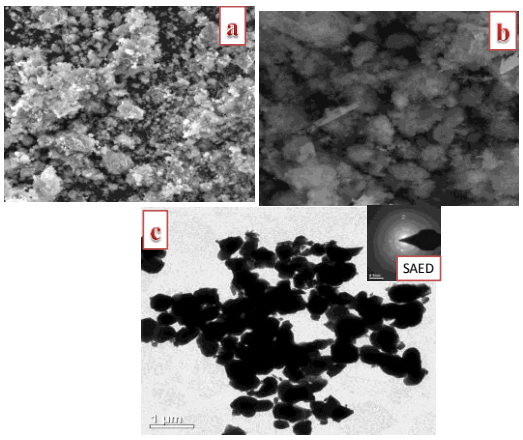

Fig. 3: SEM images of (a) as synthesized HAp, (b) HAp after adsorption and (c) TEM image of HAp with its corresponding selected area electron diffraction (SAED) as inserted.

The micrographs showed that the morphology of the prepared HAp powder is spherical in shape and were aggregated with many smaller particles. After the adsorption of the pollutants, the morphology became distorted as the particles agglomerated upon the adsorption of the pollutants and became bigger. The TEM micrograph of the prepared HAp as listed in Fig.3c with its corresponding SAED pattern as inserted. The result reveals that the as-prepared HAp powder contains spherical crystals of length varying from 15 to 35 nm and width varying from 4 to 12 nm. Analysis of the SAED revealed spotted and non-continuous rings suggesting partly crystalline grains.

Adsorption Study

Effects of Contact Time and Initial Contaminants Concentration

The time-dependent evaluation of Zn(II) ions and RY4 dye adsorption was examined by varying the contact time in the range of 5 – 240 min as presented in Fig.4. The results showed that the removal of Zn(II) ions and RY 4dye by the HAp adsorbent took place in two different steps with a quick phase in first 30 mins followed by a slow increase until the equilibrium was reached at 120 mins of contact time. There was no further appreciable increase of adsorption quantity after 120 min, and as such a contact time of 120 min was selected for further experiments. This phenomenon was due to the fact that a large number of vacant surface sites were available for adsorption during the initial stage, and as the reaction proceeds, the vacant site on the surface becomes difficult to fill up because of the repulsive forces between the solute molecules on the solid and bulk phases [19-20]. Fig. 4 also showed that the adsorption of pollutants increased with increasing initial concentration of pollutant with maximum adsorption at initial pollutant concentration of

240 mg/L. At high initial concentration of pollutant, the gradient between the solution sample and the center of particle enhances pollutant residue diffusion through the adsorbent. Initial concentration study is essential due to the fact that it can strongly affect the adsorption kinetics and more specifically, the mechanism that controls the overall kinetic coefficient [20].

Effect of Solution pH

Solution pH plays vital role most especially on the adsorption capacity by influencing the chemistry of both the contaminant and the adsorbent in aqueous medium The P_{ZPC} of the HAp powder was obtained to be 6.75 as shown in Table 1. According to Mall *et al*. [21], adsorptions of cations are favour at pH higher than $P_{ZPC,}$ while anions are favour at pH lower than P_{ZPC}. As shown in Fig.5a, when the solution pH was increased from 3.5 to 5.5, the percentage adsorption increased from 74.58 to 96.13 % for Zn(II) ions, while an increase in the pH of the dye solution from 3.5 to 6.5 show that the percentage adsorption increased sharply from 55.67 to 92.88 %. Since the surface of the adsorbent is expected to be positively charge at pH lower than P_{ZPC}, electrostatic attraction exists between the positively charged surface of the adsorbent and the anionic RY4 dye. In the adsorption of Zn(II) ions, deprotonation of the adsorbent surface at higher pH results in electrostatic attraction between the negatively charged adsorbent surface and the positively charged zinc ions. It was observed that at a higher solution pH, the adsorption capacity decreased which could be attributed to the fact that precipitation start to occur thus leading to the reduction in adsorbate uptake at higher pH value [3].

Effect of HAp Concentration

The effect of the amount of HAp on adsorption of Zn(II) ions and RY4 is as shown in Fig. 5b. The results showed that the percentage of contaminant adsorbed increased rapidly with increasing the dosage of HAp until maximum adsorption was attained at 0.04 g. The reason for this phenomenon was that, increased in adsorbent concentration provides more surface area for the pollutant and the amount retained by gram of the adsorbent increased.

Kinetic Mechanism of Adsorption

The adsorption mechanism of Zn(II) ions and RY4 dye onto HAp was investigated by using the pseudo-first-order, pseudo-second-order, Elovich and intra-particle diffusion models. The equations for these models are summarized in Table 2, while the details are as explained elsewhere [22-24]. The plots of Q_t against t from the least square fit method were used to estimate the values of the parameters as presented in Fig. 6, while the physical parameters are as listed in Table 3.

Test of Kinetic Fitness

The best fit among the kinetics models were tested by the sum of error squares (SEE, %) given by [24]:

$$\%\ \text{SSE} = \sqrt{\frac{((Q_{(\exp)} - Q_{(Cal)})/Q_{\exp})^2}{N-1}} \times 100 \qquad (4)$$

Where N is the number of data points.

Table 2: Kinetic models

Kinetic name	Kinetic model	Parameter
pseudo-first-order	$Q_t = Q_e(1-e^{-k_1 t})$	Q_e and k_1
second-first-order	$Q_t = \frac{k_2 Q_e^2 t}{1+k_2 Q_e t}$	Q_e and k_2
Elovich	$Q_t = \frac{1}{\beta} In(\alpha\beta \times t)$	α and β
intra-particle diffusion	$Q_t = K_{id} t^{0.5} + C_i$	K_{id} and C_i

The correlation coefficient and the rate constant values from the first-order model ranged from 0.986 to 0.997 and from 0.038 to 0.054 $mins^{-1}$ for Zn(II) ions, while that of RY4 dye range from 0.988 to 0.998 and from 0.051 to 0.093 $mins^{-1}$ respectively. The experimental adsorption capacity (Q_e) values were in conformity with the calculated adsorption capacity ($Q_{eCal.}$), which mean that the main rate determining step was physisorptions for the adsorption of both Zn(II)

ions and RY4 dye. From the second-order kinetic model, values of the theoretical adsorption capacity were not in good conformity with the experimental values, though the correlation coefficients values were close to unity thus suggesting the non suitability of the pseudo-second-order kinetic model. More also, the relatively high values of %SSE for second-order model when compared with those for first-order model (see Table 3) which also corroborate the fact that the pseudo-second-order model didn't fit the adsorption. From the Elovich model, values of the correlation coefficient (R^2) model ranged from 0.995 to 0.997 for Zn(II) ions and from 0.995 to 0.998 for RY 4dye, which suggests the applicability of this kinetic model for the adsorption process.

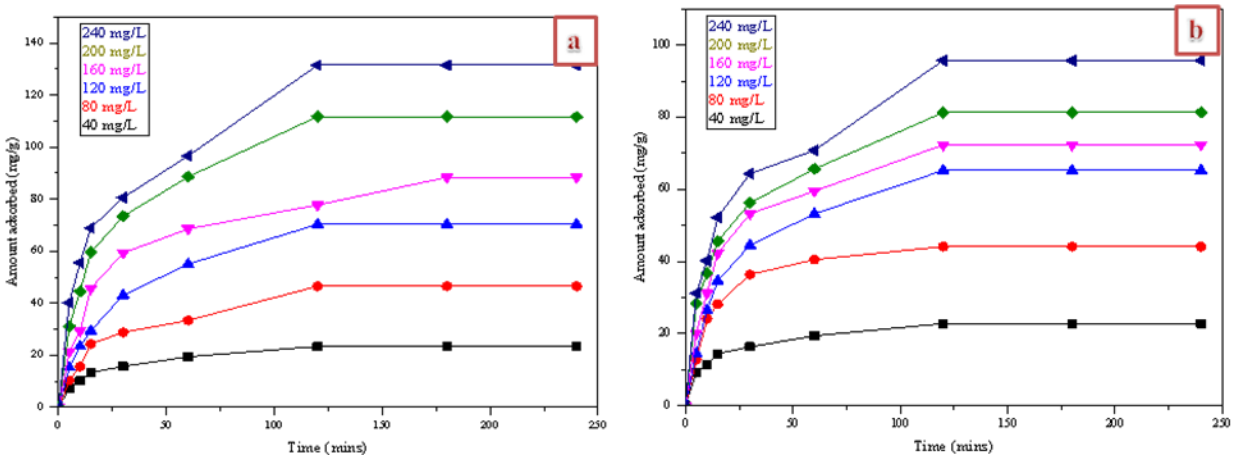

Fig. 4: Effects of contact time and initial pollutant concentration on the adsorption of (a) Zn(II) ions and (b) RY4 dye by HAp (Conditions: adsorbent dosage of 0.04 gL^{-1}; temperature 45 °C; pH of 5.5 and 6.5 for Zn(II) and RY4 dye respectively)

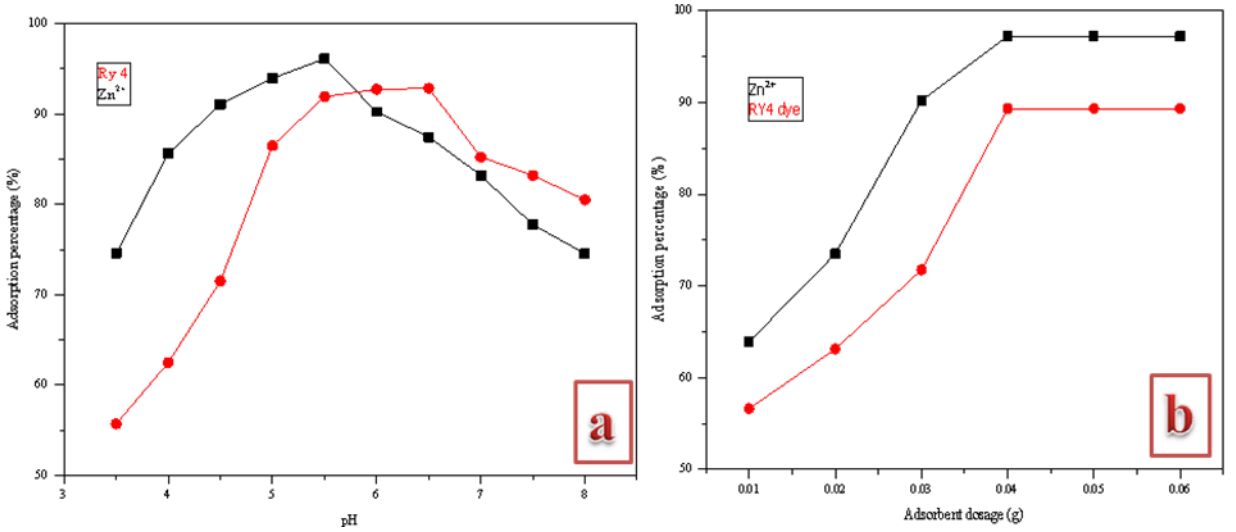

Fig. 5: Plots of the effects of (a) solution pH of Zn(II) ions and RY4 dye adsorption on HAp and (b)

Effect of adsorbent dosage on the adsorption of Zn(II) ions and RY4 by HAp (Conditions: contact time of 120 mins; temperature 45 °C)

It was further observed that the values of α (i.e. adsorption rate) increased with the pollutant concentration, while the desorption rate constant (β) decreased thus indicating strong chemical bond between the adsorbate and the various functional groups present on the surface of the HAp [24]. Evaluation of the intra-particle diffusion model reveals that the curves show a multi-linearity for the adsorbate, which suggests that the adsorption process involves more than one kinetic stage (or sorption rates). The values of R^2 ranged from 0.971 to 0.978 for Zn(II) ions and from 0.953 to 0.975 for the dye. The value of K_{id} was observed to have increased with the initial pollutant concentration which could be as result of the resistance of the surface boundary to the raise in driving force with the concentration gradient.

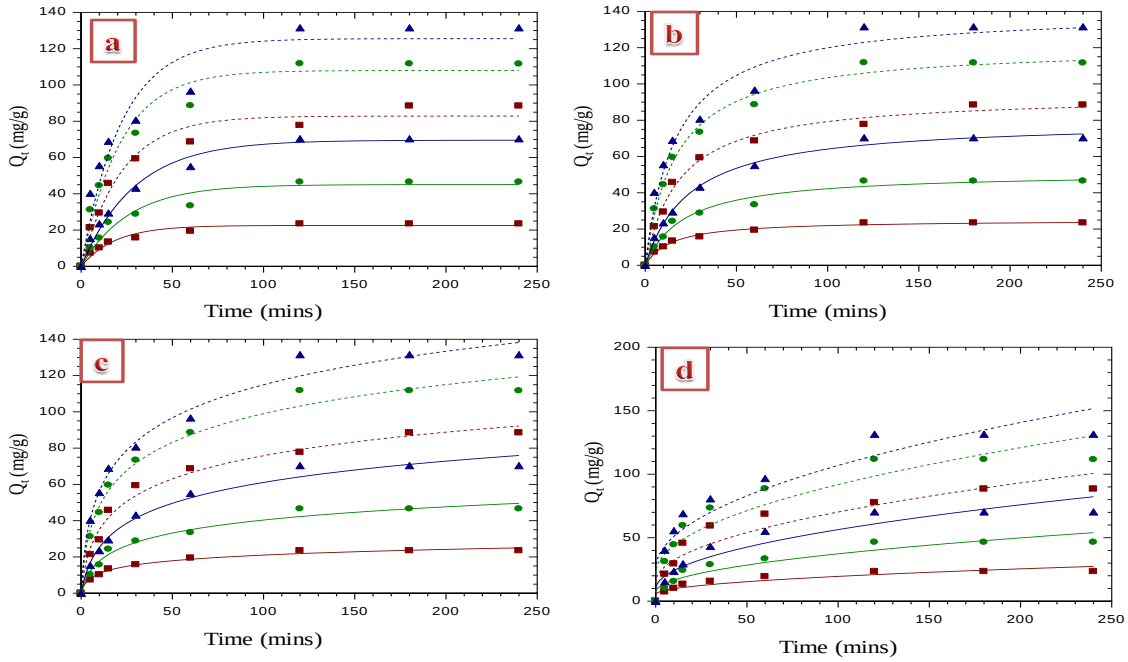

Fig. 6: Plots of (a) pseudo-first order, (b) pseudo-second-order, (c) Elovich and (d) Intra-particle diffusion kinetic models for the adsorption of Zn(II) ions on hydroxyapatite adsorbent.

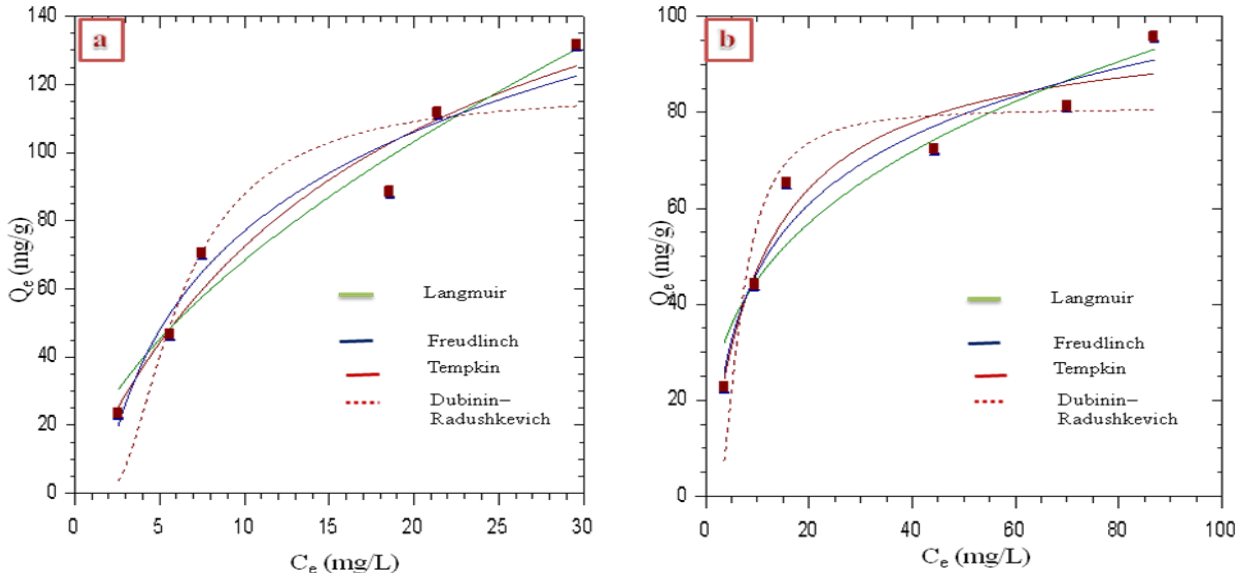

Fig. 7: Plots of Langmuir, Freundlich , Tempkin and Dubinin-Radushkevich adsorption isotherms on the adsorption of (a) Zn(II) ions and (b) RY4 dye on HAp powder

Table 4: Kinetic parameters for the adsorption of Zn(II) ions and RY4 by HAp

		Zn(II) ion						RY4 Dye					
Pseudo-first order	C_o (mg/L)	40	80	120	160	200	240	40	80	120	160	200	240
	$Q_{e\ exp}$ (mg g^{-1})	23.40	46.50	70.31	88.40	111.60	133.40	22.78	44.10	65.25	72.30	81.30	95.70
	$Q_{e\ cal}$ (mg g^{-1})	22.53	45.07	69.54	82.84	107.95	131.27	21.63	42.63	64.17	69.76	77.66	90.80
	k_1 (min^{-1})	0.054	0.038	0.038	0.045	0.047	0.045	0.072	0.093	0.040	0.056	0.056	0.051
	R^2	0.993	0.990	0.997	0.994	0.993	0.986	0.991	0.998	0.998	0.996	0.991	0.988
	%SSE	0.012	0.010	0.004	0.021	0.011	0.015	0.017	0.011	0.005	0.012	0.015	0.017
Pseudo-second order	$Q_{e\ cal}$ (mg g^{-1})	24.99	51.24	79.86	93.91	120.88	140.26	23.00	45.814	72.728	78.673	87.515	103.95
	$k_2 x\ 10^4$ (g $mg^{-1}min^{-1}$)	2.80	9.10	5.00	5.80	4.90	4.20	4.440	2.980	6.790	8.50	7.95	5.89
	R^2	0.998	0.996	0.999	0.998	0.998	0.995	0.998	0.999	0.999	0.999	0.997	0.995
	%SSE	0.023	0.034	0.045	0.021	0.028	0.022	0.009	0.013	0.038	0.029	0.025	0.027
Elovich													
	α (mg (g min)$^{-1}$)	4.483	4.520	5.730	10.166	15.942	15.942	6.846	9.014	11.245	13.850	16.700	18.000
	β (g mg^{-1})	0.219	0.093	0.058	0.053	0.043	0.037	0.263	0.151	0.066	0.070	0.065	0.053
	R^2	0.997	0.995	0.996	0.997	0.997	0.997	0.998	0.995	0.995	0.995	0.998	0.997
Intra-particle diffusion	K_{1d} (mg g^{-1} $min^{-0.5}$)	5.229	6.979	9.260	14.816	21.626	25.203	6.455	10.184	14.645	16.335	19.108	20.131
	C_1(mg g^{-1})	1.429	3.032	4.711	5.541	7.019	8.170	1.299	2.380	4.276	4.429	4.880	5.847
	R^2	0.971	0.976	0.977	0.974	0.974	0.998	0.967	0.953	0.971	0.966	0.972	0.975

Adsorption Isotherms

Adsorption equilibrium isotherms are normally used to describe the distribution of adsorbate (pollutant) molecules between the liquid and the solid phases at equilibrium. In this study, Langmuir, Freundlich, Tempkim and Dubinin-Radushkevich (D-R) adsorption isotherms were used to evaluate the adsorption data and are summarized in Table 4, while the details are as explained elsewhere [24,26-28].

Table 4: Isotherm models for the study of HAp in the removal of Zn(II) ions and RY4 dye

Isotherm name	Isotherm model	parameter
Langmuir	$Q_e = \frac{Q_o b C_e}{1 + b C_e}$	Q_o and b
Freundlich	$Q_{eq} = K_F C_e^{1/n}$	K_F and n
Tempkin	$Q_e = \frac{RT}{b_T} In a_T C_e$	A_T and B_T
Dubinin–Radushkevich	$Q_e = Q_m e^{-\beta \varepsilon^2}$	Q_m and E

The non-linear plots of Q_e against C_e for Langmuir, Freundlich, Tempkin and D-R isotherms for Zn(II) ions and RY 4 dye adsorption are shown in Fig. 7a and 7b respectively, which were used to evaluate the physical parameters as presented in Table 5. The correlation factors R^2 (0.992, 0.992, 0.992 and 0.976) for Zn(II) ions and (0.993, 0.990, 0.994 and 0.993) for RY4 dye obtained from Langmuir, Freundlich, Tempkin and D–R models confirm the applicability of these models and suggest good agreement between theoretical values and experimental results. The maximum monolayer adsorption capacity, Q_{max}, from Langmuir equation is 200.286 and 99.051 mg/g for Zn(II) ions and RY4 dye respectively. The value of the separation factor (R_L) obtained was less than unity which implies that the adsorption process is favourable [24-25].

From the Freundlich isotherm, the values of K_F obtained were 17.367 and 20.880 mg/g for zinc ions and RY4 dye respectively with adsorption affinity values (n) > 1 which further corroborate the favourable nature of the adsorption process. For the D-R isotherm, the values of adsorption constants as obtained for Zn(II) ions and RY 4 dye are 117.753 and 80.892 mg/g for Q_m and 0.309 and 0.2805 kJ/mol for E respectively. Since the value of E is less than 8 kJ/mol, the adsorption is governed by physical [24-26].

The values of the maximum binding energy of adsorption obtained from the Tempkin isotherm equally suggest favourable adsorption process.

Table 5: Isotherm Parameters for Zn(II) ions and RY4 dye Adsorption onto HAp

		Zn(II) ions	RY4 dye
Langmuir	**Q_{max} (mg/g)**	200.286	99.051
	R_L	0.057	0.092
	b (mg/L)	0.0694	0.04119
	R2	0.992	0.993
Freundlich	**K_F (mg/g)(mg/L)$^{-1/2}$**	17.367	20.880
	n	1.681	2.986
	R^2	0.992	0.990
Tempkin	**α_T (L/g)**	0.627	0.976
	b_T (J/mol)	59.090	121.017
	R^2	0.992	0.994
Dubinin–Radushkevich	**Q_m (mg/g)**	117.753	80.892
	E (kJmol^{-1})	0.309	0.2805
	R^2	0.976	0.993

Effect of Temperature and Thermodynamic Study

An increase in temperature leads to an increase in the rate of particles diffusion across external boundary layer and internal pores of the adsorbent due to decrease in the viscosity of solution [24]. Furthermore, an increase in temperature may result in swelling effect within

the internal structure of the adsorbent thus enhancing pollutants penetration [29].

Thermodynamic parameters such as change in free energy (ΔG°), enthalpy (ΔH°) and entropy (ΔS°) of adsorption system were evaluated using the Van't Hoff equation [28]:

$$InK_C = -\frac{\Delta H^o}{RT} + \frac{\Delta S^o}{R} \qquad (5)$$

Where K_C is the equilibrium constant which expresses the relationship between the amounts of pollutant adsorbed (Q_e) in mg/g and the equilibrium concentration (C_e) in mg/L.

The free energy change of the adsorption reaction was estimated by:

$$\Delta G^{\theta} = -RTInK_e \qquad (6)$$

Where ΔG° is standard free energy change (kJ/mol/K), R is the ideal gas constant (8.314 J/mol /K) and T is the absolute temperature (K). The thermodynamic values are presented in Table 6.

Table 6: Thermodynamic parameters for the adsorption of Zn(II) ions and RY4 dye by HAp

Zn(II) ions					
T (K)	**K_D**	**ΔG (kJ/mol)**	**ΔH (kJ/mol)**	**ΔS (kJ/mol)**	**R^2**
303	1.022	-55.673	4.92×10^6	51.123	0.9397
308	1.103	-250.642			
313	1.1813	-433.54			
318	1.399	-888.334			
RY4 dye					
T (K)	**K_D**	**ΔG (kJ/mol)**	**ΔH (kJ/mol)**	**ΔS (kJ/mol)**	**R^2**
303	1.037	-92.2006	3.99×10^6	41.803	0.9866
308	1.111	-268.849			
313	1.247	-574.35			
318	1.309	-711.857			

The values of enthalpy change (ΔH) and entropy change (ΔS) as obtained are 4.92×10^6 kJ/mol and 51.123 kJ/mol for Zn(II) ions and 3.99×10^6 kJ/mol and 41.803 kJ/mol for RY4 dye respectively. The evaluations of free energy and enthalpy changes revealed that the adsorption process was spontaneous and endothermic in nature. The negative values of the free energy change (ΔG), suggest the feasibility of the process and spontaneous nature of the adsorption of zinc ions and reactive yellow 4 dye onto HAp while the positive value of the enthalpy change (ΔH) inferred the endothermic nature of the adsorption process. The positive value of entropy change (ΔS) revealed the good affinity of zinc ions and RY4 dye toward the adsorbent (HAp) and indicate increased randomness at the solid/solution interface during the adsorption process.

Conclusions In this present study, the adsorption ability of HAp powder for Zn(II) ions and reactive yellow 4 dye from aqueous

solutions was investigated under different experimental conditions such as effect of contact time, initial pollutants concentrations, adsorbent dosage, temperature and solution pH. The adsorption of Zn^{2+} and RY4 were best described with first-order kinetic model. Langmuir, Freundlich, Tempkin and D–R models were used to describe the adsorption behaviour of Zn^{2+} and RY4 by HAp. Thermodynamic evaluation confirmed that the adsorption process was spontaneous, feasible and endothermic in nature. Thus, HAp powder can serve as an excellent adsorbent for the removal of zinc ions and reactive yellow 4 dye in remediation applications.

Acknowledgement

The authors would like to thank the Department of Science and Technology, Government of India for supporting this work through RTF-DCS (DST) fellowship awarded to E. A. Ofudje. Authors equally thank the technical staff of Central Instrumentation Facility (CIF) of CSIR-Central Electrochemical Research Institute, Indian for their supports during the analysis of the results.

References

1. B. B. Chavan (2013). Health and Environmental Hazards of Synthetic Dyes. Available at:http://www.fibre2fashion.com/industryarticle/printarticle.asp?article_id=4708&page=1. Accessed: 01/03/2017.
2. D. D. Asouhidou, K. S. Triantafyllidis, N.K. Lazaridis, K.A. Matis, S.S. Kim and T. J. Pinnavaia (2009). Sorption of Reactive Dyes from Aqueous Solutions by Ordered Hexagonal and Disordered Mesoporous Carbons. Microporous and Mesoporous Materials, 117, 1-2,257–267.
3. A.I. Adeogun, E.A. Ofudje, M.A. Idowu and S.A. Ahmed (2012). 'Kinetic, thermodynamic and Isotherm Parameters of Biosorption of Cr(VI) and Pb (II) ions from Aqueous Solution by Biosorbent Prepared from Corncob biomass. Indian Journal of Inorganic Chemistry, 7, 3,119-129.
4. E. H. Mohammadine, R. Abdelmajid, L. My Rachid, M. Rachid and S. Nabil (2014). Use of Fenton reagent as advanced oxidative process for removing textile dyes from aqueous solutions. Journal of Material Environmental Science, 5, 3, 667-674.
5. S.A. Abo-Farha (2010). Comparative study of oxidation of some azo dyes by different advanced oxidation processes: Fenton, Fenton-like, photo-fenton and photo-fenton-like. Journal of American Science, 6, 10, 128-142.
6. J.C. Igwe and A.A. Abia (2007). Adsorption kinetics and intraparticulate diffusivities for bioremediation of Co(II), Fe(II) and Cu(II) ions from waste water using modified and unmodified maize cob. International Journal of Physical Sciences, 2, 119-127.
7. K. Conrad and H.C.B. Hansen (2007). Sorption of zinc and lead on coir. Bioresource Technology, 98, 89–97.
8. E.A. Ofudje, A.O. Awotula, G.V. Hambate, F. Akinwunmi, S.O. Alayandeand O.D. Olukanni (2017). Acid Activation of Groundnut Husk for Copper Adsorption: Kinetics and Equilibrium Studies. Desalination and Water Treatment. 86, 240–251.
9. Mohan D., Singh K.P., Singh V.K., (2006), Trivalent chromium removal from wastewater using low cost activated carbon derived from agricultural waste material and activated carbon fabric cloth. Journal of Hazardous Materials, B135, 280–295.
10. T.J. Webster, E.A. Massa-Schlueter, J.L. Smith and E.B. Slamovich (2004). Osteoblast response to hydroxyapatite doped with divalent and trivalent cations. Biomaterials, 25, 11, 2111-2121.
11. L. Kai and C.T. Sie (2011). Preparation and Characterization of Isotactic

Polypropylene Reinforced with Hydroxyapatite Nanorods. Journal of Macromolecular Science, Part B: Physics, 50, 1983-1995.

12. N. Neelakandeswari, G. Sangami and N. Dharmaraj (2011). Preparation and Characterization of Nanostructured Hydroxyapatite Using a Biomaterial. Synthesis and Reactivity in Inorganic, Metal-Organic, and Nano-Metal Chemistry, 41, 513-516.

13. S.S. Mehdi, T. K. Mohammad, D.K. Ehsan and J. Ahmad (2013). Synthesis methods for nanosized hydroxyapatite with diverse structures. Acta Biomaterialia, 9, 7591–7621.

14. N. Monmaturapoj (2008). Nano-size hydroxyapatite powders preparation by wet-chemical precipitation route. Journal of Metals, Materials and Minerals, 18, 1, 15-20.

15. E.H. Ezechi, S.R. A. bin Mohamed Kutty and Malakahmad, M.H. Isa (2015). Characterization and optimization of effluent dye removal using a new low cost adsorbent: equilibrium, kinetics and thermodynamic study. Process Saf. Environ. Prot. 98, 16−32.

16. Q.Q. Ding, X.J. Zhang, Y. Huang, Y.J. Yan and X.F. Pang (2015). In vitro cytocompatibility and corrosion resistance of zinc doped hydroxyapatite coatings on a titanium substrate. Journal of Material Science, 50, 189–202.

17. D. Gopi, E. Shinyjoy and L. Kavitha (2014). Synthesis and spectral characterization of silver/magnesium co-substituted hydroxyapatite for biomedical applications. Spectrochim. Acta, Part A, 127, 286–291.

18. H. Yong, Z. Xuejiao, M. Huanhuan, L. Tingting, Z. Ranlin, Y. Yajing and P. Xiaofeng, (2015). Osteoblastic cell responses and antibacterial efficacy of Cu/Zn co-substituted hydroxyapatite coatings on pure titanium using electrodeposition method. Royal Society of Chemistry, Advance, 5, 17076–17086.

19. H.H. Sokker, N.M. El-Sawy, M.A. Hassan and B.E. El-Anadouli (2011). Adsorption of crude oil from aqueous solution by hydrogel of chitosan based polyacrylamide prepared by radiation induced graft polymerization. Journal of Hazardous Materials, 190, 359–365

20. F. Yuan, G. Ji-Lai, Z. Guang-Ming, N. Qiu-Ya, Z. Hui-Ying, N. Cheng-Gang, D. Jiu-Hua and Y. Ming (2010). Adsorption of Cd (II) and Zn (II) from aqueous solutions using magnetic hydroxyapatite nanoparticles as adsorbents. Chemical Engineering Journal, 162, 487–494

21. I. D. Mall, V. C. Srivastava, N. K. Agarwal (2006). Removal of Orange- G and Methyl Violet dyes by adsorption onto bagasse fly ash-kinetic study and equilibrium isotherm analyses. Dyes Pigments, 69,210–223.

22. S. Lagergren (1898). About the theory of so-called adsorption of soluble substance. Kung Sven. Veten. Hand, 24, 1–39.

23. Y.S. Ho and G. McKay (1998). Kinetic models for the sorption of dye from aqueous solution by wood. Journal of Environmental Science Health Part B: Process Saf. Environ. Prot. 76, 4,183–191.

24. A.I. Adeogun, M.A. Idowu, E.A. Ofudje, S.O. Kareem and S.A. Ahmed (2013). Comparative biosorption of Mn(II) and Pb(II) ions on raw and oxalic acid modified maize husk: kinetic, thermodynamic and isothermal studies. Applied Water Science, 3, 167–179.

25. I. Langmuir (1918). The adsorption of gases on plane surfaces of glass, mica and platinum. Journal of America Chemical Society, 40:1361–1403.

26. H.M.F. Freundlich (1906). Über die adsorption in lösungen, Z. Phys. Chem. 57, 385-470.

27. M.J. Tempkin and V. Pyzhev (1940). Recent modifications to Langmuir isotherms. Acta Physiochim. *USSR* , 12, 217-222.

28. M. Dogan and M. Alkan (2003). Adsorption kinetics of methyl violet onto perlite. Chemosphere, 50, 517-528.